Journal of Engineering Science and Technology
Vol. 21, No. 2 (2026) 436 - 467

DEVELOPMENT AND ASSESSMENT OF NOVEL THERMOELECTRIC GENERATOR BY THERMAL ENERGY SCAVENGING TECHNIQUES IN HVAC SYSTEM

FIRAS BASIM ISMAIL[1,2,3,*], NIZAR F. O. AL-MUHSEN[4], THABIT SULTAN MOHAMMED[5], MAGD AHMED ABDULQAHER[1], HUSSEIN A. KAZEM[6], MIQDAM T. CHAICHAN[7], MOHAMMAD SHALBY[8], AHMAD SALAH[9]

[1]Smart Power Generation Research Centre, Institute of Power Engineering (IPE), Universiti Tenaga Nasional, Kajang, 43000, Malaysia
[2]Faculty of Engineering, Sohar University, PO Box 44, Sohar, PCI 311, Oman
[3]Engineering College, Al-Bayan University, Baghdad, Iraq
[4]Technical Instructors Training Institute, Middle Technical University, Baghdad, Iraq
[5]Computer Technical Engineering Department, Al-Qalam University, Kirkuk, Iraq
[6]UNESCO RCQE Chair in Emerging Renewable & Sustainable Energy Technologies, Sohar University, PO Box 44, Sohar, PCI 311, Oman
[7]Energy and Renewable Energies Technology Center, University of Technology Iraq
[8]Department of Mechanical Engineering, Al-Hussein Bin Talal University, Maan 71110, Jordan
[9]Department of Electrical Engineering, Al-Hussein Bin Talal University, Maan, Jordan
*Corresponding Author: Firas@uniten.edu.my

Abstract

This work introduces a novel thermoelectric generator (TEG) module designed to harvest energy from residual heat around cylindrical HVAC pipes. Unlike conventional flat TEGs, the module adopts a polygonal shape that wraps efficiently around pipe surfaces. It consists of stacked layers (each 4 mm thick) with 2.0 mm spacing to enhance heat transfer while maintaining a compact design. A dedicated coupling method ensures strong thermal contact. To improve performance, various semiconductor materials were evaluated under typical HVAC conditions. Experimental results show that each TEG layer can generate between 0.01176 and 0.18802 W, equivalent to about 2–30 W per meter of pipe circumference under steady operation. With temperature differences of 10 °C – 30 °C, the system achieves around 8% conversion efficiency. An integrated energy management system with battery storage stabilizes the output and powers components such as a condenser fan using only harvested energy. Overall, this study provides a practical and scalable solution for converting HVAC waste heat into clean electricity, offering improved design, material selection, and system integration compared to previous approaches.

Keywords: ANSYS, Energy harvesting, HVAC, Seebeck coefficient, Semiconductor internal resistance, Thermoelectric generators.

1. Introduction

With increasing focus on environmental concerns and energy conservation in the present world, energy efficiency enhancement of the Heating, Ventilation and Air Conditioning (HVAC) systems has become an important goal for business and environmental requirements due to their huge energy consumption. Energy efficiency in HVAC systems cannot be overemphasized in the contemporary world [1]. HVAC systems have a critical role in regulating comfort indoors in buildings for residential, commercial and industrial purposes [2]. Practically, there is a significant energy loss when the HVAC systems are not accurately controlled, which could severely affect the used energy bills and resources. Additionally, the large energy consumption of the HVAC systems means a greater carbon footprint for these systems [3]. Accordingly, optimizing the performance of the HVAC systems has become one of the strong tools for relieving climate change and reducing GHG emissions [4]. This objective could be reached via different methods comprising the structure's development in the system's design, adopting the latest emerging technologies in the HVAC systems' energy management [5].

Global warming and climate change have emerged as serious issues that need to be addressed worldwide. Besides, due to the global energy crisis caused by conventional energy shortage and increased demand for electricity, scientific researchers and the relevant industry have paid greater attention to using renewable energy sources and adopting more efficient energy consumption management strategies. The waste heat recovery of thermal systems has been considered a promising method to enhance the performance of some thermal systems. This recovery process can be carried out directly or indirectly through heat exchangers [6]. Therefore, TEGs have emerged as a promising technology to convert waste heat into electricity. These generators operate silently, can be scaled, with no moving parts, and generate power whenever a temperature gradient exists. Figure 1 shows classifications of TEGs usage. One substantial source of waste heat is HVAC systems that release a significant amount of energy, especially through condensers. The exhaust airflow from All-Air HVAC systems also dissipates the unused heat making it suitable for cooling applications. In this context, this study proposes an innovative design for a TEG module, tailored to the cylindrical configuration of HVAC pipes, overcoming the limitations of existing rectangular modules.

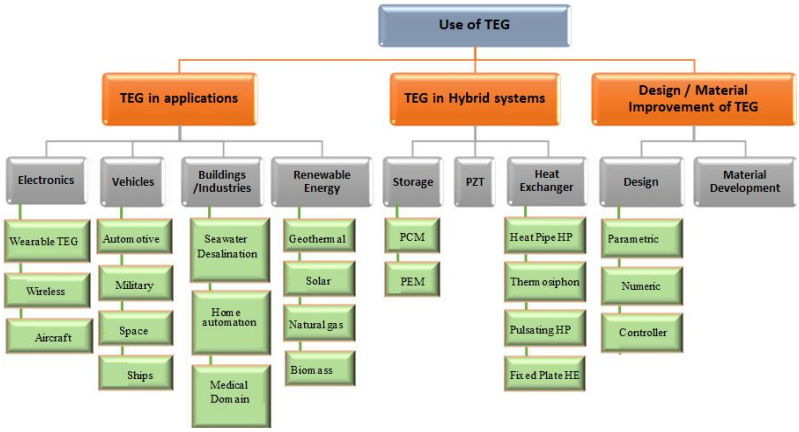

Fig. 1. TEGs usage classification [7].

Ambient energy harvesting has grown substantially recently [8]. In response to the recent energy crisis, both industries and researchers have pivoted towards a more holistic energy management approach, particularly by enhancing the efficiency of energy systems [9]. The conversion of vibrational energy into electrical energy entails integrating strains, magnetic fields, or electrostatic forces onto piezoelectric materials. Thermal energy restoring methods mean that the dissipated heat from mechanical systems such as that stemming from hot surfaces or exhaust gases and then converted into useful energy [10]. Evaluating their effectiveness can be best accomplished through power density which can be defined as the power output per unit volume or area. Because the waste energy is cost-free and its fuel-independent nature of ambient energy, its spatial efficiency becomes paramount. Gkoumas et al. [11]investigated the feasibility of extracting electrical energy from airflow-induced vibrations using piezoelectric materials. The authors examine the potential for integrating energy harvesting technology into HVAC systems. Besides, Fiorentini et al. [12] introduced a hybrid model predictive control strategy for a residential HVAC system. Their study incorporates photovoltaic-thermal (PVT) energy generation and phase change material (PCM) thermal storage. The authors presented a control scheme that could manage energy usage to fairly incorporate PVT generation and PCM storage. The performance improvement in the residential HVAC system was the main object of using both renewable power generation and thermal energy storage.

LeBlanc [13] highlighted the relationship between the properties of the material and system engineering for TEG applications. The authors reported that the synergy between material science and utilizing the TEGs is essential to enhance the overall power effectiveness. Different types of waste heat recovery procedures were presented and analysed [14]. They explained the importance of waste heat efficiency and overall energy management and provided an overview of the technology used in waste heat recovery and the overall state of advancement in the field. Mona et al. [15] proposed a system aimed to utilize thermoelectric power generation from air conditioning units. Eight series connected TEGs soldered onto an aluminium heat sink with one side of the TEGs heated. The cold side of the TEGs was soldered to three water-cooled aluminium blocks that faced downwards. Their results showed that in the case of a cooling load of 100 kW, a flat plate measuring 40×40 cm² can produce 90 W of electrical power. The link between TEG power generation and condensation rate was contingent upon thermostat temperature, elucidated and expressed. Additionally, multiple linear models for TEG power generation were formulated concerning influential independent variables, thus suggesting the potential application of TEG-based energy harvesting from air conditioners. Aridi et al. [7] reviewed the current state of TEGs, covering their advancements and challenges. They examined heat recovery techniques for maximizing efficiency. In terms of selecting the right materials, the conversion efficiency and the strategies of thermoelectric design are investigated. The study slightly contributed by highlighting the applicability of these generators in utilising waste heat for generating extra power [16].

Since HVAC systems contribute a major fraction of the waste heat during air conditioning, transferring and utilizing such heat through automated heat exchangers can greatly enhance air conditioning efficiency. Different TEG techniques and progressive control methods have been aimed at decreasing energy waste and improving the sustainability of HVAC systems. Ma et al. [4] used solar thermal

energy in HVAC pipes by using highly heat conductance material aluminium pipes which can make benefiting the cost-free energy in supplementing heating processes viable. This not only reduces energy consumption but also adds up to sustainability initiatives. Yang et al. [17] described a novel work that incorporates power harvesting from fluid in HVAC pipes. When piezoelectric material is integrated in some places, the motion of fluids converts mechanical energy into electrical energy and caters to the power requirements of HVAC systems.

This research aims to introduce a novel and pioneering design for harvesting energy. The suggested system is conducted experimentally and numerically by applying TEGs to HVAC thermal pipes. This work used a tailored cylindrical TEG module design since HVAC pipes have a cylindrical configuration. This innovative design integrates multiple TEG modules onto the pipes coherently, effectively forming a layered assembly of TEGs. What distinguishes this design is the unique side in terms of reusing the TEG units already present in a rectangular shape and adapted in an octagonal shape that fits with the current copper HVAC systems. Such a dedicated design means that a set of layers of multiple TEG units can be linked directly to the curved surface of the tube, thus facilitating the useful extraction of thermal energy offered from the infrastructure of the cylindrical pipeline. This ability cannot be achieved in a traditional flat standard design. This concept will continue to use traditional TEG units; however, it will clarify their spatial composition and mechanical packaging to capture the best hues on curved surfaces that have not been considered in previous designs that target flat/rectangular installations.

2. Methodology

2.1. Energy harvesting system design

In this subsection, a new design was proposed to create a waste heat recovery system from HVAC pipes in an air-conditioning unit. Commonly available rectangular TEGs measure 40 mm × 40 mm with a thickness of approximately 5 mm [18]. Multiple TEG modules within this assembly are interconnected to enhance power output. Because the standard designs of commercial TEGs do not fit HVAC pipes due to geometric disparities, the TEG module arrangement in this study was customized into a closed-loop polygonal shape suitable for cylindrical pipes. Selection of appropriate materials for this assembly involves comparing the three best P-type and N-type semiconductors. ANSYS Workbench simulation for nine configurations of the proposed design was performed, pitting each of the top three N-type materials against the other three P-type materials, such as modules such as DesignModeler for geometry creation, meshing for mesh generation, and mechanical for structural analysis. For each permutation, simulations were conducted under temperature gradients of 10, 20, 30, and 40 °C, with specific voltages tied to material properties and temperature gradients. Current values, power generation, heat input, and efficiency of the design and materials were attained. The sequence and primary stages of the used methodology are shown in Fig. 2.

The 2.0 mm interfaces between stacked TEG layers are supposed to permit thermal isolation and sustain a temperature gradient between individual layers. But the consideration made by the reviewer regarding the possibility of thermal bridging with these gaps is accurate, because unintentional conductive or convective heat transfer routes may decrease effective T and impair TEG

performance. These gaps are deliberately left in the developed design and are probably bridged or insulated using appropriate materials (e.g., air gaps, thermally insulating fillers) to reduce the effects of bridging, but this again should be experimentally verified. It is suggested that in the future experimental and simulation studies will involve comprehensive thermal resistance and bridging tests of the interlayer spacing to adjust the gap size and insulation strategy to trade-off between mechanical stability and thermal action.

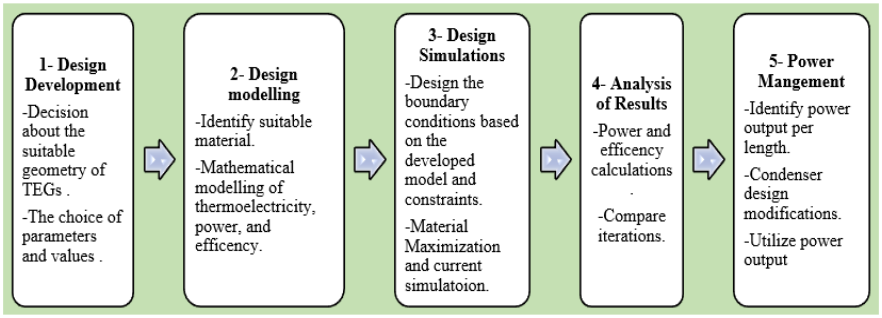

Fig. 2. Research methodology stages.

2.2. Proposed design

The proposed design aims to harness the heat dissipated from an HVAC unit's condenser by using TEGs to produce electricity, particularly at the copper pipes that exit the compressor and enter the condenser. This research focuses on TEG technology better suited for cases with a consistent temperature gradient. In previous designs for similar cases, TEG modules were conventionally rectangular. However, in this study, a new adaptation is required due to the cylindrical shape of the copper pipes where the TEGs will be attached. The proposed new design reshapes the TEG module instead of modifying the heat source. In a standard HVAC setup, heated refrigerant traverses the cylindrical copper pipes in route to the condenser. As illustrated in Fig. 3, the proposed design encompasses thermoelectric materials enveloping these pipes in a polygenic shape, allowing the TEG module to establish contact with surfaces of differing temperatures.

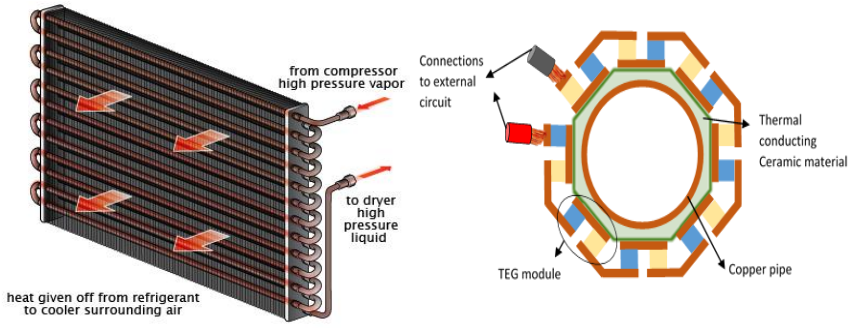

(a) **(b)**

Fig. 3. (a) Condenser setting, (b) Schematic of the developed design.

2.3. Design constraints

The formulated design for the air conditioning-based TEG module is bound by several limitations:

- Ensuring sufficient surface area for TEG module installation on the copper pipes.
- Achieving an optimal heat transfer rate to establish distinct hot and cold surface temperatures [18].

Given the structure of the condenser, the copper pipes are already configured with multiple turns to enhance surface area for improved heat exchange as shown in Fig. 3(a). Additionally, a fan operates continuously to cool the refrigerant by directing airflow onto the pipes. These pipes are integrated within the condenser. Besides, as the proposed design is directly mounted onto the copper pipes, rather than onto supplementary metal sheets as seen in prior literature, slight adjustments are needed for the condenser. This involves increasing the condenser's height to accommodate the added pipe layers. Furthermore, the airflow from the fan serves the dual purpose of cooling the outer surface of the copper pipes. When attaching the TEG module to the copper pipes, this airflow will cool down the TEG module's cold side. Consequently, the existing dynamics of the condenser inherently provide the necessary limitations, which the developed design effectively harnesses.

2.4. Design parameters and simulation strategy for optimized performance

The parameters of the formulated design are contingent upon the geometry of the copper pipes, which typically span diameters ranging from 6 to 24 mm. In this specific design, the chosen diameter for study is 24 mm, and all other aspects will be adjusted accordingly. The parameters encompass:

- The dimensions of the TEG module to be affixed to the ceramic material.
- The polygon's side count on the ceramic material, which will attach to the pipes.

The dimensions of the TEG module encompass measurements for both semiconductors and the upper and lower copper plates. The lower copper plate, experiencing higher temperatures, exhibits a rectangular shape, while the upper cold plate has a contoured form to conform to the design, depicted in Fig. 4(b). The chosen dimensions for the front view of the TEG module in the developed design are shown in Fig. 4(a), with each part maintaining a thickness of 5 mm. The geometry of the TEG module arrangement was meshed to be discretized into finite elements for analysis. Figure 4 includes information on the generated mesh settings for the proposed module design such as element type and size.

The final parameter to address involves selecting the appropriate semiconductor material. This choice is related to the temperature range in which the TEG module will function, given that the condenser's highest temperature could change between 40 to 80 °C. Within this range, the optimal semiconductor choices are N-type Bi-Te and P-type Bi-Sb-Te, particularly for temperatures under 100 °C, as illustrated in Fig. 5 [19].

Thermoelectric materials possess the ability to convert electrical energy into thermal energy and vice versa. The functionality of thermoelectric materials revolves around two factors: the Seebeck effect and its inverse, the Peltier effect. The Seebeck

effect involves the generation of an electrical voltage through a temperature gradient across a thermoelectric material.

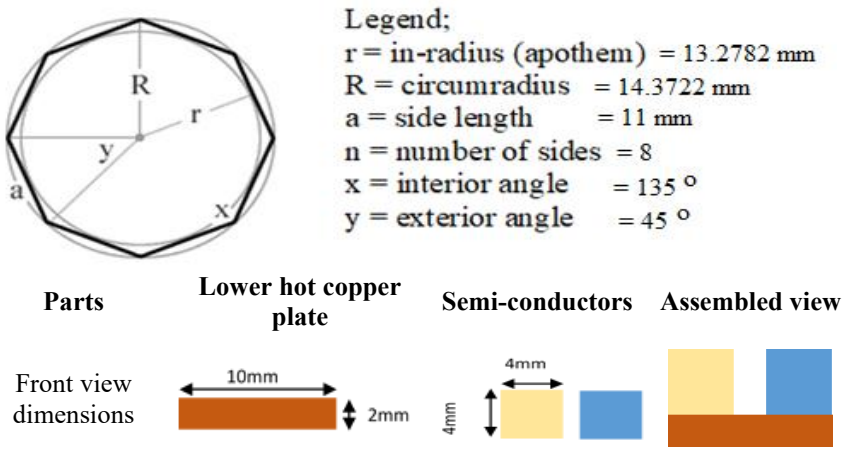

Fig. 4. (a) Individual TEG module geometry, (b) Polygon parameters and dimensions for the developed TEG module.

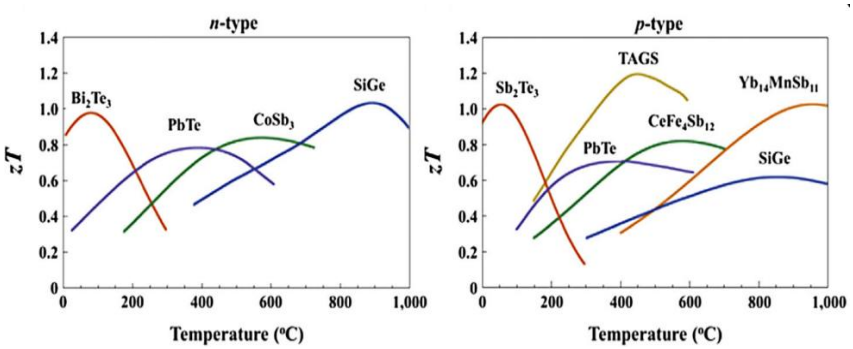

(a) **(b)**

Fig. 5. A summary of established state-of-the-art thermoelectric bulk materials with high ZT: (a) n-type materials and (b) p-type materials [19].

Evaluating the effectiveness of a thermoelectric material involves computing the dimensionless figure of merit (ZT). ZT values are computed for a range of potential materials by applying the formula:

$$ZT = \frac{S^2\sigma}{K}\,T, \tag{1}$$

where, S is the Seebeck coefficient, σ is the electrical conductivity, k is the thermal conductivity, and T is the temperature of the semiconductor.

This process helps identify the top three materials with the highest ZT values, which are then considered for subsequent simulations. Table 1 illustrates the ZT calculations for the finest three P-type and N-type semiconductors.

Table 1. The calculated ZT values for the best P-type and N-type semiconductors.

Semiconductor	The material used	The value of ZT
The best three P-type semiconductors	$Bi_{0.4}Sb_{1.5}Te_3$ with CNT added	1.47
	$Bi_{0.45}Sb_{1.55}Te_{3.02}$ with graphene added	1.40
	$Bi_{0.45}Sb_{1.55}Te_{3.02}$ with Si_3N_4 added	1.38
The best three N-type semiconductors	Bi_2Te_3 with SiC added	1.04
	$Bi_2Te_{2.7}Se_{0.3}$ with Al_2O_3 added	0.99
	$Bi_2Sb_{2.7}Se_{0.3}$ with CNT added	0.98

Based on the values of ZT shown in Table 1, the chosen materials that will be adopted in this research exhibit improved ZT values when combined with other components. An enhancement of up to 47% is achieved.

The paper acknowledges the need to study the thermal stresses caused by the coefficient of thermal expansion (CTE) variations between the TEG ceramic substrates, semiconductor materials, and copper tubes. This misalignment can create stresses during thermal cycling, which might lead to issues like delamination, cracks, or mechanical failures. A thermomechanical simulation of a TEG assembly on cylindrical copper tubes is suggested and is carried out with the help of finite element analysis (FEA). This will model stresses and strains within normal operating temperature ranges (say 27 to 67 °C, as in the experiment) and thermal gradients. Material selection strategies to minimize CTE mismatch should also be addressed, e.g., by choosing ceramics and semiconductors that have compatible or intermediate CTEs or by introducing compatible dielectric layers/interfacial materials to absorb stress. Experimental validation of the study is proposed to be conducted by using thermal cycling to observe the mechanical stability of the TEG layers attached to the copper tubes and identify delamination or cracking. - See the appropriate literature on thermal stress management on TEG units or other thermo-mechanical laminated devices to validate their reliability.

An actual emphasis needs to be put on the resistance of the vibrations created by the compressors and fans, detecting the vibrations and mechanical dynamic loading as the essential stressors in the HVAC system caused by the compressor and fan operation. Suggest vibration testing of prototype TEG units attached to pipes, at frequencies and amplitudes appropriate to real operating conditions, to determine structural stability and connection dependability. Talk about mechanical design characteristics that improve vibration resistance, e.g., flexible system, shock-absorbing mounts, or solid enclosure design. Suggest a fatigue study in place of operating cycles to determine service life when subjected to vibration. Suggest adding damping materials/vibration isolators between the TEG and pipes to reduce the dynamic stresses.

While the conduction-dominated heat transfer problems in simple geometries can often be analytically solved, there are several reasons for employing CFD software in such cases. First and foremost, CFD provides a versatile and comprehensive approach that allows us to account for more complex boundary conditions, intricate geometries, and additional heat transfer mechanisms beyond conduction. Furthermore, CFD simulations enable a detailed investigation of the flow patterns and temperature distributions within the system, providing a more thorough understanding of the physical processes involved. This allows for the exploration of transient effects, turbulence, and convective heat transfer that may

be present even in seemingly simple configurations. In this study, the simulation process is conducted in ANSYS workbench®.

The ANSYS simulation platform delivers the broadest suite of best-in-class simulation technology and unifies it with custom applications, CAD software and enterprise business process tools such as PLM. ANSYS workbench has a built-in thermoelectric model that can be used for the simulation process. The three main stages of the simulation are as follows:

- Build the developed design in ANSYS design modular.
- Input material properties, such as the Seebeck coefficient, resistivity and thermal conductivity to the developed design.
- Input the constraints of temperature, voltage and insulation while measuring the output current, power can then be calculated by following equation:

$$Power = Voltage \times Current \quad (2)$$

For convenience, the simulation process will include the TEG module only, without the flow of refrigerant in the pipes nor the flow of air from the fan of the condenser. Since the temperature that will affect the hot surface of the TEG, is of the most concern, the hot temperature constraint will be added at the hot side copper plate of the TEG module instead. The paper explicitly states that the simulation was conducted without modelling the refrigerant flow or airflow from the condenser fan. Instead, constant temperatures were applied directly to the hot and cold sides of the thermoelectric generator unit to simplify the process and focus on the effects of conduction and electrical heat. This approach simplifies the model to isolate and evaluate the thermoelectric generator material properties and unit design without the added complexity of fluid dynamics. Similarly, the simulation will add another cold temperature constraint at the cold side of the TEG module instead of simulating the flow of air from the fan of the condenser. The simulation procedure will then be repeated at different temperature ranges with different material inputs. The adopted materials are the three best "P-type and N-type semiconductors" as shown in Table 1. Moreover, the ceramic material will not be included in the simulation, as its function is to transfer the heat from the copper pipe to the hot surface of the TEG module and at the same time provide electrical insulation between the hot copper plate of the copper pipe. Figs. 6(a) and (b) illustrate a comparison between the developed design and the simulated respectively.

The simulation procedure is repeated at different temperature ranges and different material inputs. The three N-type materials and three P-type materials considered in this study lead to nine possible permutations. Each permutation is simulated with temperature gradients (ΔT) ranging from 10 to 40°C at an increment of 10°C each time. The cold side temperature is assumed at room temperature of 27°C for each case, while the hot side temperature will be 37, 47, 57 and 67°C considering the temperature gradients of 10, 20, 30 and 40°C respectively. These temperature values can be explained by the fact that these ranges were determined depending on reasonable and workable HVAC condenser operating conditions. The maximum temperature of the condenser may be up to 80 and allowing a reasonable range of 37 to 670 °C, the range used in the simulation is within range. This implies that the temperatures were selected using the known or even the predicted HVAC operating conditions facilitated by scientific literatures that include discussions on the performance of thermoelectric material below 100 °C [20, 21]. The temperature

of the cold face, 27 °C, is the temperature of the fan-cooled room air, and the actual convective cooling effect is imposed indirectly as a boundary condition. Although this makes the detailed capture of forced convection heat transfer fluctuations more difficult, the intent was to give a simple performance prediction. Computing convection and fluid flow was not yet in the scope of this phase of the simulation but is deemed significant in future improvements.

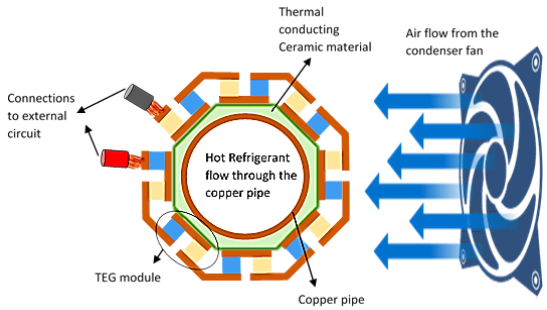

(a)

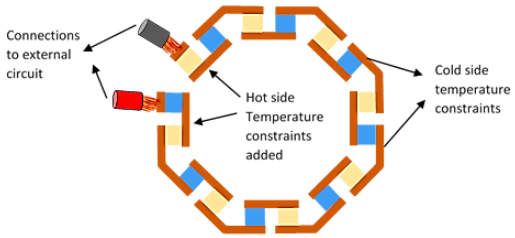

(b)

Fig. 6. (a) actual working condition of the developed TEG module design, (b) simulated working conditions of the developed TEG module design.

This paper relies on constant temperature limits on TEG surfaces as a working approximation to capture the usual operating conditions based on research and experimental evidence related to HVAC systems. This step is taken to avoid the complexity of integrating thermal models with fluid flow models of refrigerant and air dynamics, which are more demanding in terms of computing power and complex system modelling. These problems also address the necessity to take into account the arrangement of condensers and tube sizes in order to choose a plausible range of temperatures and to take into account certain thermal resistance phenomena in the chosen temperature range but treat it as neglected or part of the chosen temperature range. This simplification is useful because it allows the performance metrics of thermoelectric generators (TEGs) (voltage, current, power, and efficiency) to be evaluated in an environment of constant temperature gradients. Application of gradients of temperature (10-40 °C) falls within the practical operating limits of HVAC condenser tubes. They are, however, aware that omitting the reality of real convective heat transfer and interface resistances can result in utopian temperature differences and, therefore, idealistic power outputs.

Thus, the results reported are to be understood as the highest or best possible performance, giving positive evidence of principle but not exact field projections.

A summary of the simulation iterations is shown in Table 2, where the properties of the adopted semiconductor material based on the nine possible permutations, are tabulated. It's evident from the data in Table 2 that a total of 36 different experiments were performed. The variability in outcomes across iterations can be attributed to the inherent sensitivity of the model to initial conditions, parameter settings, or other factors influencing the iterative process. The model's convergence or divergence in each iteration contributes to the overall robustness and reliability of the results. It is emphasized that any adjustments made in subsequent iterations enhance the model's accuracy and convergence.

Table 2. Properties of the adopted semiconductor material based on the nine possible permutations.

Iteration number	Temperature gradient (ΔT) /°C	P-Type material name			N-Type material name		
		S	**σ**	**k**	**S**	**σ**	**k**
1	10,20,30,40	$Bi_{0.4}Sb_{1.5}Te_3$ with CNT			Bi_2Te_3 with SiC		
		235	19.2	0.68	-138	9.1	0.85
2	10,20,30,40				$Bi_2Te_{2.7}Se_{0.3}$ with Al_2O_3		
					-156	8.7	1.13
3	10,20,30,40				$Bi_2Sb_{2.7}Se_{0.3}$ with CNT		
					-163	12.3	0.93
4	10,20,30,40	$Bi_{0.45}Sb_{1.55}Te_{3.02}$ with graphene			Bi_2Te_3 with SiC		
					-138	9.1	0.85
5	10,20,30,40				$Bi_2Te_{2.7}Se_{0.3}$ with Al_2O_3		
		231	17.5	0.79	-156	8.7	1.13
6	10,20,30,40				$Bi_2Sb_{2.7}Se_{0.3}$ with CNT		
					-163	12.3	0.93
7	10,20,30,40	$Bi_{0.45}Sb_{1.55}Te_{3.02}$ with Si_3N_4			Bi_2Te_3 with SiC		
		219	16.2	0.82	-138	9.1	0.85
8	10,20,30,40				$Bi_2Te_{2.7}Se_{0.3}$ with Al_2O_3		
					-156	8.7	1.13
9	10,20,30,40				$Bi_2Sb_{2.7}Se_{0.3}$ with CNT		
					-163	12.3	0.93

To calculate the power output of a TEG module, several fundamental principles of thermoelectricity are applied. Firstly, the Seebeck coefficient, known as thermoelectric power, of a material determines its ability to generate an electric voltage in response to a temperature gradient. It quantifies the voltage produced per unit temperature difference across the material. A larger temperature differential results in higher voltage generation and increased power output. By considering the aforementioned fundamental principles, along with the geometric and material properties of the proposed TEG module, it is possible to calculate the power output of the TEG system. Mathematical models based on these principles are developed to predict the voltage, current, and power generated by the TEG module under specific operating conditions. These models facilitate the optimization of TEG design and performance for various applications, including energy harvesting from waste heat in HVAC systems. The voltage output of one TEG module can be calculated based on Eq. (3).

$$V = S\,x\,\Delta T \tag{3}$$

where S is the average Seebeck coefficient, ΔT is the temperature difference between the surfaces (TH-TC). If several TEG modules are connected in series, then Equation 1 can be reformed as Eq. (4) [20].

$$V = n \times S \times \Delta T \tag{4}$$

where n is the number of TEG modules. When a load is connected to the thermoelectric TEG module, the output voltage (V) drops as a result of internal resistance. The current through the load can be calculated by Eq. (5).

$$I = \frac{n \times S \times \Delta T}{R} \tag{5}$$

where I is the generator output current in amperes, while R is the average resistance of the TEG module and the load resistance in ohms. The total heat input (QH) to the TEG module is defined in Eq. (6).

$$Q_H = (S \times T_H \times I) - 0.5 I^2 R_I + \mathrm{k}_t \times \Delta \mathrm{T} \tag{6}$$

where QH is the heat input in watts, k_t is the thermal conductance of the TEG module in Watts/K, T_H is the hot side of the TEG in K, while R_I is the internal resistance in ohms. The efficiency of the generator can be calculated from Eq. (7).

$$eff = \frac{P}{Q_H} \tag{7}$$

As shown in Table 3, S represents the Seebeck coefficient, meanwhile, σ and k are the electrical resistivity and thermal conductivity, respectively. The voltages between the sides for each case are calculated according to Equation 2. In the developed design, the number of TEG modules is n = 8, and S is the average Seebeck coefficient for the semiconductors. Values of the calculated voltages between the developed TEGs are listed in Table 3.

Table 3. Summary for voltage values for TEG iterations.

Iteration number	Avg. S in μV/°C	The voltage outcome of 8 TEG modules at different temperature gradients (ΔT)			
		V at ΔT =10 °C	V at ΔT =20 °C	V at ΔT =30 °C	V at ΔT =40 °C
1	186.5	0.01492	0.02984	0.04476	0.05968
2	195.5	0.01564	0.03128	0.04692	0.06256
3	199	0.01592	0.03184	0.04776	0.06368
4	184.5	0.01476	0.02952	0.04428	0.05904
5	193.5	0.01548	0.03096	0.04644	0.06192
6	197	0.01576	0.03152	0.04728	0.06304
7	178.5	0.01428	0.02856	0.04284	0.5712
8	187.5	0.015	0.03	0.045	0.06
9	191	0.01528	0.03056	0.04584	0.06112

The voltage value will be added at the N-Type face in the connection to the external circuit port shown in the developed design schematic shown in Fig. 7, while the other port (i.e. P-Type) will be kept at zero voltage. Current, current density and temperature distribution will then be obtained from the simulation experiments. Based on the values of current obtained, power and efficiency are calculated using Eq. (5) - Eq. (7).

To calculate the total heat input QH, internal resistance R_I and thermal conductance K_t, need to be calculated. Both values are material and geometry

dependent; therefore, an analysis of the geometry is required in order to determine these values. The R_l value can be found based on Eq. (8) [21].

$$R = \rho \times \frac{l}{A} \tag{8}$$

where: l is the length of the wire, and A is the cross-sectional area.

For the designed geometry, there are three main materials, therefore resistance of each is calculated and then added in series. From Fig. 7(a), in which the current path based on the geometry is approximated, the length of current passing through copper that will affect the resistance is 0.0236m, while it is 0.004m for each semiconductor.

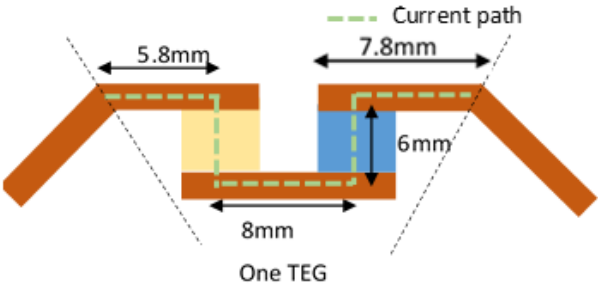

(a)

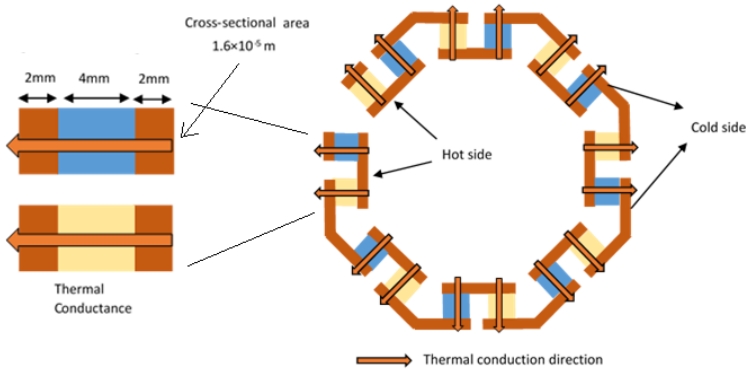

(b)

Fig. 7. (a) current path in a single TEG module, (b) thermal conduction direction in the developed TEG design.

The cross-sectional area of the copper plates is 8×10^{-6} m^2 meanwhile the cross-sectional area of each semiconductor is 1.6×10^{-5} m^2 which is used to find the values of resistances. Resistance of copper section (RC):

$$R_c = \rho_C \times \frac{l}{A} = 1.68 \times 10^{-8} \times \frac{0.0236}{8\times10^{-6}} = 4.956 \times 10^{-5}\Omega \tag{9}$$

Resistance of each semiconductor (P-Type and N-Type):

$$R_p = \rho_p \times \frac{l}{A} = \rho_p \times \frac{0.004}{1.6\times10^{-5}}\Omega \tag{10}$$

$$R_N = \rho_N \times \frac{l}{A} = \rho_N \times \frac{0.004}{1.6\times10^{-5}} \Omega \quad (11)$$

Total internal resistance R_I is the sum:

$$R_I = R_C + R_P + R_N \quad (12)$$

For the whole TEG layer (each layer has 8 TEGs), the internal resistance:

$$R_I = 8 \times (R_C + R_P + R_N) \quad (13)$$

Based on Eq. (13), the R_I value for each iteration is calculated and listed in Table 4.

Table 4. Internal resistance for each iteration.

Iteration number	Internal Resistance RI [mΩ]
1	56.9965
2	56.1965
3	63.3965
4	52.7965
5	52.7965
6	59.9965
7	50.9965
8	50.9965
9	57.3965

The other needed value to obtain is k_t. Figure 7(b) shows the approximate thermal conduction pattern and dimensions of each part of the TEG module that will conduct heat. Moreover, Eq. (14) is used to find the thermal conductance of each material.

$$K_t = k \times \frac{A}{l} \quad (14)$$

where; K is thermal conductivity, A is the area, and l is the length.

Each part in a single TEG module is made of two materials, including copper (kc) and a semiconductor. Copper is a great conductor of heat that helps the supplied heat on one side to be transferred quickly to the other side of the TEG. Therefore, there are more concerns about calculating the conductivity of the semiconductor materials, as the difference between the sides generates the voltage. Applying Eq. (14), the thermal conductance values (k_{tP}) and (k_{tN}) for both P-type and N-type semiconductor materials are calculated.

$$K_{tP} = k_p \times \frac{A_p}{l_p} = k_p \times \frac{1.6\times10^{-5}}{0.004} = k_p \times 0.004 \quad (15)$$

$$K_{tN} = k_n \times \frac{A_n}{l_n} = k_n \times \frac{1.6\times10^{-5}}{0.004} = k_n \times 0.004 \quad (16)$$

The total conductance (K_t) of a single TEG module is:

$$K_t = k_{tP} + k_{tN} \quad (17)$$

Since there are eight single TEG modules in one layer of the developed design, the total conductance of one layer of TEGs is:

$$K_t = 8 \times (k_{tP} + k_{tN}) = 8 \times (k_p \times 0.004 + k_n \times 0.004) = 0.032\ (k_p + k_n) \quad (18)$$

Based on the obtained equation $K_t = 0.032\ (k_P + k_n)$, the total conductance for each iteration is calculated and shown in Table 5.

Table 5. Thermal conductance for each iteration.

Iteration number	Thermal conductance kt in (W/℃)
1	0.049
2	0.057
3	0.052
4	0.052
5	0.061
6	0.055
7	0.053
8	0.062
9	0.056

This paper proposes a new polygonal framework of conventional rectangular TEG modules tailored to the geometry of cylindrical HVAC pipes, which actually is more complicated to assemble than flat, rectangular designs. Note that the mechanical design, fabrication, and possibly special tooling to build these polygonal modules will be precise and may increase the cost and complexity of production. State that although this work is mainly design, simulation, and proof-of-concept, a cost-benefit analysis of manufacturing complexity versus energy harvested and potential savings in energy will be done in future work. It has to be noted that tailored geometry allows enhanced thermal contact and harvesting on curved pipes, which may make such complexity potentially worthwhile to enhance energy recovery in some HVAC applications.

The present work is devoted to steady-state simulations as an initial step to assess the performance of the proposed thermoelectric generator (TEG) design and the material combinations under stable temperature gradients characteristic of the operating conditions of the HVAC condenser. With a steady-state approach, the voltage, current, power output, and efficiency can be studied in detail without further complicating the analysis with transient thermal and electrical behaviors.

It should also be acknowledged that the HVAC system in practice is exposed to dynamic and variable loads, such as start-ups, shutdowns, and varying ambient conditions, leading to unsteady power generation profiles of TEG units. These non-persistent effects are harder to monitor without more complex time-dependent modeling and integration of operating data of HVAC systems, which is not in the scope of this baseline study.

It is also intended to extend the modeling framework to transient analysis in the future, where consideration is made of variable thermal loads, varying temperature gradients, and variable environmental factors. These studies will offer further understanding of the strength, responsiveness, and realistic power production variability of thermoelectric power generation (TEG) systems operating under actual scenarios of HVAC settings.

Simultaneously, the steady-state outcomes discussed in this paper offer good initial performance indicators and information used to optimize design, key conditions to perform transient simulation, and experimental validation.

In this way, even though transient effects are necessary to give a complete account of the integration of HVAC systems with TEG, steady-state simulation outcomes allow us to provide the necessary background and show the potential of the proposed energy harvesting method in operating conditions.

2.5. TEG design

The proposed TEG module design is modelled using the ANSYS design package based on the dimensions calculated and discussed in the previous section. The front and isometric views, as well as sketching several layers of the developed TEG design, are shown in Fig. 8. Indeed, the design revolves around a solitary layer of the TEG module, a deliberate choice made to streamline the simulation and analysis procedures. This approach simplifies the estimation of power generation per unit length, drawing from the outcomes of a single-layer simulation.

(a) (b) (c)

Fig. 8. The developed TEG design (a) Front View, (b) Isometric view, (c) Several layers of the TEG module.

3. Results and Discussion

In this section, the outcomes of simulations concerning the integration of TEG modules onto the pipes of a heated air conditioning condenser will be presented. Initially, the ANSYS design modular representation of the developed design will be exhibited. Subsequently, an analysis of the power outcomes derived from simulations, encompassing distinct temperature gradients and diverse materials, will be undertaken. Based on these findings, a comparative assessment will be conducted, ultimately leading to selecting the most efficient design. Subsequent exploration will revolve around the potential applications of the design, yielding optimal outcomes, specifically for implementation within the condenser. Finally, deliberation on management strategies and other essential design parameters for the integration into condenser coils will be discussed.

3.1. Simulation results

The simulation is conducted for the nine permutations, which were discussed in the previous section and presented in Table 2. In the rest of this paper, the work related to each permutation is referred to as an iteration. As previously stated, the cold side temperature is set at room temperature of 27°C for all permutations, while the hot side temperature is 37, 47, 57 and 67°C with temperature gradients of 10, 20, 30 and 40, respectively. For each iteration, there are 5 input values, where the input to the high voltage terminal is based on the (S, σ, k) values tabulated in Table 3, while the low voltage terminal is kept at zero volts for all iterations. For all other faces in the geometry of the developed TEG module, a convection rate of 1.0 $\mu W/m^2$ is added for negligible convection. Figure 9(a) shows a sample of the constraints and boundary conditions. It shows a sample of the boundary conditions (A) of hot plate temperatures, (B) of cold plate temperatures, (C) high potential, (D) low potential, and (E) convection.

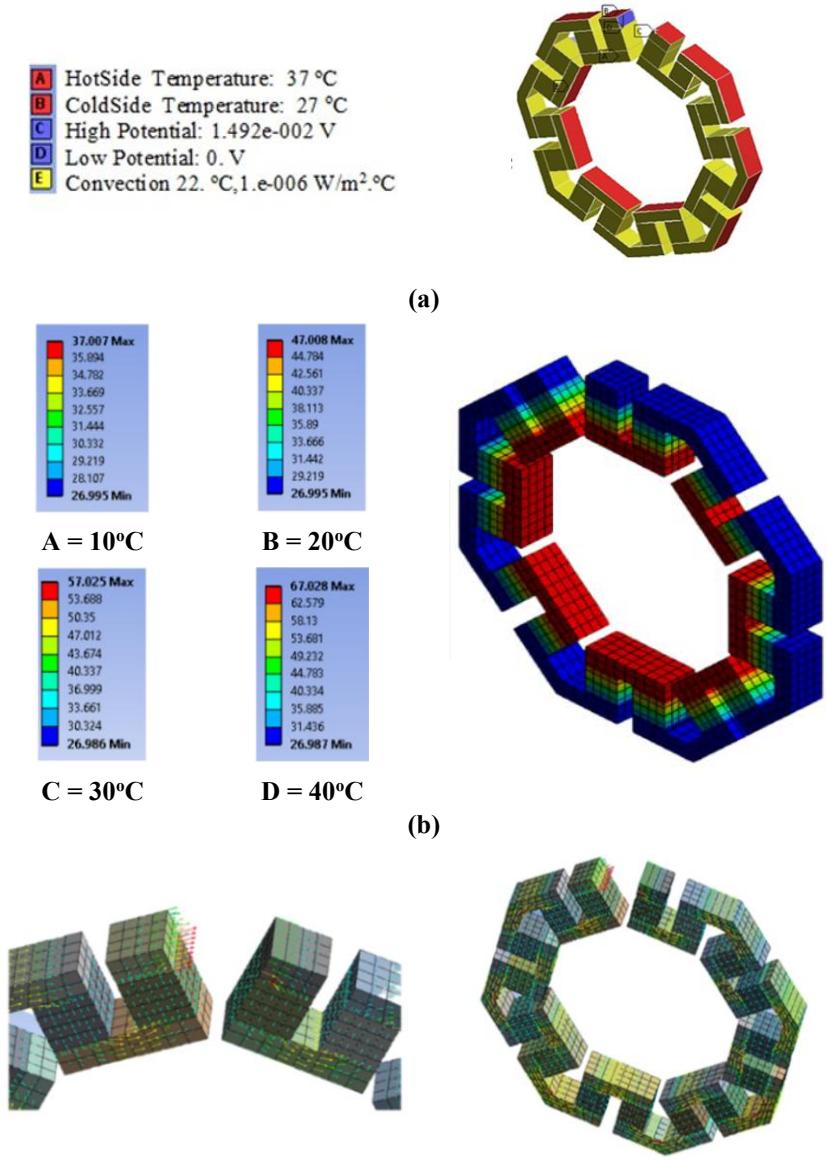

Fig. 9. (a) constraints input sample, (b) temperature distribution along the TEG module with the key index for temperature gradients of 10, 20, 30 and 40oC, (c) current distribution patterns along the TEG design.

The temperature distribution along the developed TEG module, the current density, and the current reaction are solved. The results obtained from these solutions are then used to calculate power. Figure 9(b) illustrates the temperature distribution in the designed TEG module for the temperature gradients of 10, 20, 30 and 40°C. Patterns of the current density distribution from the simulation are

found to be similar for all the worked iterations, however, with different values. A sample of the distribution pattern is shown in Fig. 9(c).

Based on the nine permutations related to the use of different semiconductor materials (P and N types), nine experiments are conducted. Among the inputs to each simulation iteration are the properties of the adopted semiconductor material based on the nine possible permutations. Before performing an iteration, further input values are required for the simulation. Within each iteration, composed of the four temperature gradients, the input values include voltage in [V], internal resistance (RI) in [mΩ], and thermal conductance (kt) in [W/^{o}C]. The outputs obtained from the ANSYS Workbench simulations, such as voltage distribution, current flow, power generation, and efficiency metrics, were illustrated in Table 6. In Table 6, the input values together with the obtained output results are shown. Output results include the obtained current values, and the calculated values of power, heat input, and efficiency.

Table 6. Input values and output results for the nine simulation iterations.

Iter. No.	Temp. grad.	Input				Output Results			
		Volt.	$S_{Avg.}$	RI	Kt	Current	Power	$Heat_{tot,\ input}$	Eff.
	°C	V	μV/℃	mΩ	∫/℃	Amp	W	W	%
1	10	0.01492	186.5	56.997	0.049	0.65426	0.009762	0.51563	1.89
	20	0.02984				1.3084	0.039043	1.00930	3.87
	30	0.04476				1.9624	0.087837	1.48103	5.93
	40	0.05968				2.6163	0.15614	1.93083	8.09
2	10	0.01564	195.5	56.197	0.057	0.6954	0.01088	0.59856	1.82
	20	0.03128				1.3907	0.04350	1.17266	3.71
	30	0.04692				2.0858	0.09787	1.72232	5.68
	40	0.06256				2.7808	0.17396	2.24756	7.74
3	10	0.01592	199	63.397	0.052	0.62745	0.00999	0.54623	1.83
	20	0.03184				1.2548	0.03995	1.07000	3.73
	30	0.04776				1.882	0.08988	1.57132	5.72
	40	0.06368				2.5091	0.15978	2.05021	7.79
4	10	0.01476	184.5	52.797	0.052	0.6883	0.01016	0.54686	1.86
	20	0.02952				1.3765	0.04063	1.07125	3.79
	30	0.04428				2.0645	0.09142	1.57318	5.81
	40	0.05904				2.7524	0.1625	2.05267	7.92
5	10	0.01548	193.5	52.7965	0.061	0.73261	0.01134	0.63978	1.77
	20	0.03096				1.4651	0.04535	1.25405	3.62
	30	0.04644				2.1974	0.10204	1.84285	5.54
	40	0.06192				2.9295	0.18139	2.40618	7.538
6	10	0.01576	197	59.997	0.055	0.7459	0.01176	0.57886	2.03
	20	0.03152				1.4916	0.04702	1.12729	4.17
	30	0.04728				2.2372	0.10577	1.64530	6.43
	40	0.06304				2.9826	0.18802	2.1329	8.82
7	10	0.01428	178.5	50.997	0.053	0.69998	0.01000	0.55624	1.79
	20	0.02856				1.3998	0.03998	1.09000	3.67
	30	0.04284				2.0995	0.08994	1.60128	5.62
	40	0.05712				2.799	0.15988	2.09010	7.65
8	10	0.015	187.5	50.997	0.062	0.74678	0.01120	0.64919	1.73
	20	0.03				1.4934	0.044802	1.27274	3.52
	30	0.045				2.2399	0.10796	1.87067	5.78
	40	0.06				2.9861	0.17917	2.44300	7.33
9	10	0.01528	191	57.397	0.056	0.66524	0.01016	0.58669	1.73
	20	0.03056				1.3304	0.04066	1.15052	3.53
	30	0.04584				1.9954	0.09147	1.69150	5.41
	40	0.06112				2.6603	0.16260	2.20966	7.36

Nine iterations of simulation are done to obtain the current density vector distribution along the TEG module in [A/m^2]. The graphs for the four temperature gradients, accompanied by the key index, are obtained from all nine different iterations. However, due to space limits, only graphs for the simulated current density in TEG for the first iteration are shown in Fig. 10.

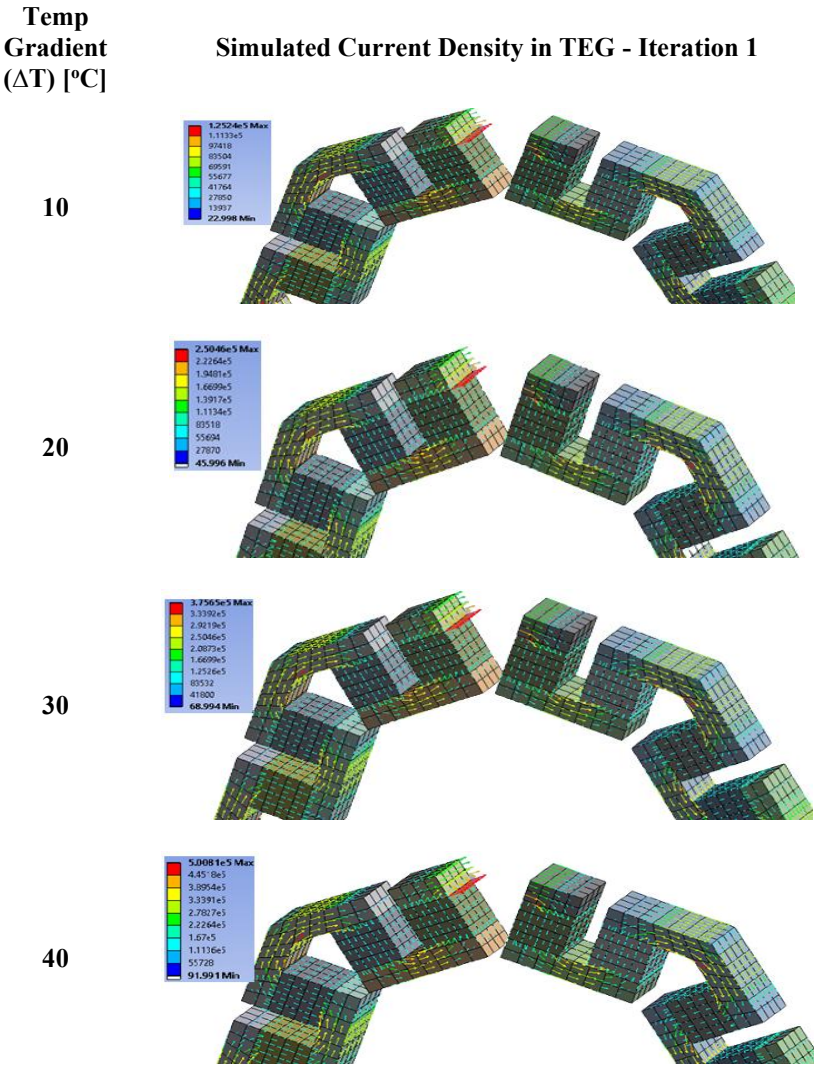

Fig. 10. Current density for iteration 1.

The comparison of currents produced for all iterations against the temperature gradients is shown in Fig.11(a). As anticipated, the currents generated by the TEG module exhibit a proportional relationship with the temperature gradient. The highest current output, reaching 2.98A, is observed during iteration number 8, corresponding to the maximum temperature gradient. Conversely, the minimum current output, measured at 0.62A, occurs during iteration 3 at the lowest temperature gradient.

Figure 11(b) illustrates the comparison of power produced for all iterations across the four temperature gradients. The power values generated by the TEG module correlate directly with the temperature gradients, with the power gradient escalating as the temperature gradient increases. The maximum power output of 0.18802W is achieved during Iteration 6, coinciding with the maximum temperature gradient. In contrast, the minimum power output, recorded at 0.15614W, is observed during Iteration 1 under the minimum temperature gradient. Additionally, Fig. 11(c) presents a comparison of efficiencies for all nine iterations against the temperature gradients. The efficiency values exhibited by the TEG module also demonstrate a proportional relationship with the temperature gradients. The highest efficiency of 8.82% is attained during Iteration 6, aligning with the maximum temperature gradient. Conversely, the minimum efficiency values, measured at 1.73%, are recorded during Iterations 8 and 9, corresponding to the lowest temperature gradients.

To compare the current study with the literature results reported by Jouhara et al. [22] evaluated the performance of a TEG-based waste heat recovery system for internal combustion engine exhaust gas. They reported similar trends in power generation with temperature gradients, observing higher power output at larger temperature differentials. The results of their study corroborate the findings of the current research in terms of the relationship between temperature gradients and power generation. Alexander and Sadiku [23] provided a comprehensive review of recent progress in thermoelectric materials, including their properties and applications. While their study focused more on material science aspects, the fundamental principles and behaviours of thermoelectric materials discussed align with the theoretical framework of the current research. The insights provided by the authors supported the selection and optimization of thermoelectric materials in the current study. Moreover, Demir and Dincer [24] investigated the performance of a thermoelectric generator module for automotive exhaust gas heat recovery. Their study analysed power generation under various operating conditions, including temperature differentials and flow rates. The results obtained by this study were consistent with the findings of the current research, providing validation for the performance trends observed in TEG-based energy recovery systems.

The results from the simulation showed that the best combination of materials came from iteration 6. The semiconductor materials used for this simulation are:

- P-Type: Bi0.45Sb1.55Te3.02 with graphene
- N-Type: $Bi_2Sb_{2.7}Se_{0.3}$ with CNT

This combination produces the best power outcomes, ranging from 0.01 to 0.188W for minimum temperature gradients to maximum temperature gradients, respectively. Likewise, iteration 6 results in the best efficiency values ranging from 2% to 8.8% for minimum temperature gradients to maximum temperature gradients, respectively. The efficiency of TEG modules is not as important as their power density, which is the power generated per unit area or volume. This is true because TEG is a waste energy heat scavenging technique, which is not similar to the conventional generator, and it does not run by using any type of fuel. The more power obtained from less space, the more effective the TEG module is. Practically, a thermoelectric TEG power module used for power generation has certain similarities to a conventional thermocouple. Semiconductor devices, which form

the core material in TEGs, can withstand temperatures up to 150°C in some cases. In HVAC Systems, the high temperatures will mostly be less than 100°C.

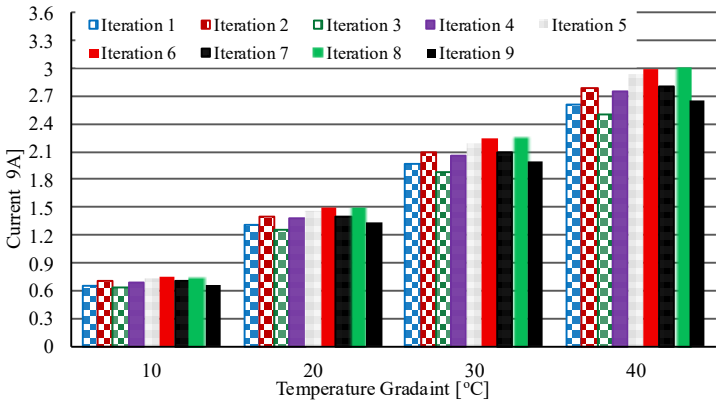

(a)

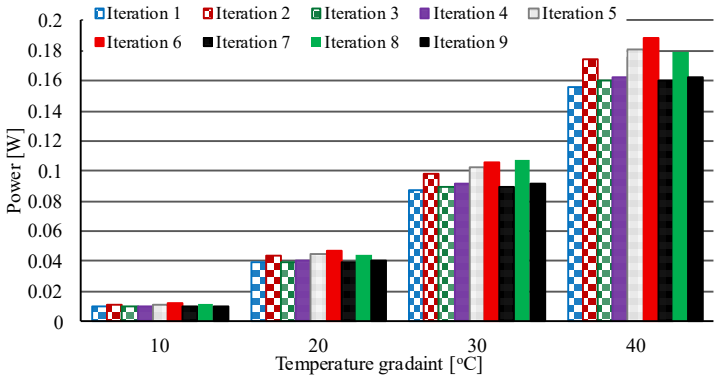

(b)

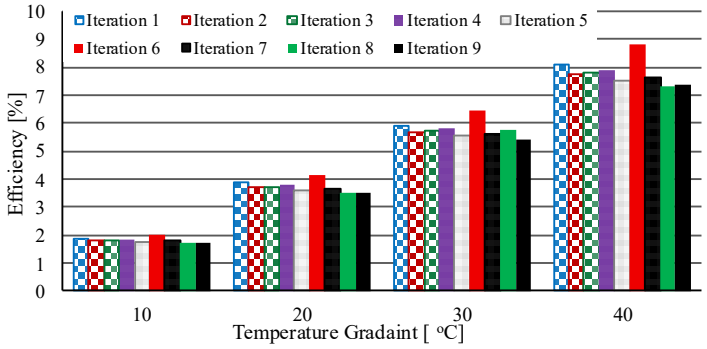

(c)

Fig. 11. (a) currents, (b) power, (c) efficiencies vs temperature gradients of all iterations constituting the 36 simulation experiments.

3.2. Case study

In this paper, simulation techniques are adopted and applied to enhance the design materials and then evaluate the produced power. Simulation of how to effectively

convert and manage the generated power into a practical and useful form is also analysed and presented. The actual implementation of the project is planned for continuation in a separate phase. Besides, real-time experimental data will be obtained by conducting practical experiments and obtaining real-time experimental data to substantiate the outcomes of the simulation.

This paper recognizes the fact that this existing simulation framework presupposes constant material properties (Seebeck coefficient, electrical resistivity, and thermal conductivity) using literature values of the selected semiconductor materials and composites. Such properties are necessarily subject to variability since manufacturers are not always accurate, and they should change with temperature outside the nominal ranges considered and may degenerate between operational cycles. The resulting variability may affect the modelled thermoelectric performance (voltage, current, power output, and efficiency) by changing the important dimensionless figure of merit (ZT) and internal values of resistance.

To overcome this weakness, a formal uncertainty and sensitivity analysis of the material properties that were employed in the ANSYS simulations will be included in future work. This may be carried out by providing probabilistic distributions on the key inputs due to experimental evidence or literature-reported ranges and by running Monte Carlo simulations or parametric sweeps. These will measure the spread of the uncertainties with the simulation model and test the robustness and reliability of predicted TEG performance measures with realistic material variability.

In addition, material properties under temperature variation and the interface contact resistance, which are currently ignored, will also be incorporated to reflect more detailed variations and their influence on device efficiency. This optimization will be used to tune the selection of material and design optimization with confidence intervals to enhance design margins with realistic manufacturing and operation conditions.

To conclude, although the present simulation illustrates the perfect maximum performance of the proposed TEG designs, it forms the basis of the future detailed uncertainty quantification and validation experiments to further improve the predictive power of the system and its applicability in industry. This route is consistent with the best practice in the modelling of thermoelectric devices and such that the system design may appropriately adapt to changes in the real world.

In this subsection, a system to manage this output power is proposed, and a scheme is developed. Through this scheme, the output power from the TEG module can be exploited. The power values obtained from the simulation represent the outcome of a single layer of the TEG. Each layer is considered to have a thickness of 4 mm, so it is practical to develop an index of power per pipe length or by the number of layers mounted in a pipe. Recall that a gap of 2 mm is applied between each layer and the other, then, a layer with the gap takes about 6 mm of pipe length. With these facts in mind, one meter of the pipe will have about 166 layers of TEGs. A representation of the TEG module layers mounted onto a cylindrical copper pipe is shown in Fig. 12(a). Furthermore, the power index for the optimized material, showing the power ratings per meter of length with the corresponding number of layers, is 166 per meter as shown in Table 7.

There is a scientific explanation for why heat build-up (or thermal bridging) between closely stacked TEG layers with 4 mm thickness and a 2.0 mm gap could reduce the effective temperature difference (ΔT) across the thermoelectric modules:

- Thermal Resistance and Heat Transfer Pathways: The efficiency and power output of TEGs depend strongly on maintaining a significant temperature gradient (ΔT) between their hot and cold sides. When multiple TEG layers are stacked with small gaps (2.0 mm spacing), these gaps can provide unintended thermal conduction and/or convection pathways, creating a "thermal bridge." This reduces the thermal resistance that is supposed to isolate each layer's hot and cold sides.
- Thermal Bridging and Heat Bypass: The 2.0 mm gaps between the layers could allow heat to bypass the thermoelectric material through conduction (via supporting structural materials or residual gas in the gap) or convection (if air or another fluid fills the gap and circulates). This results in leakage of heat from the hot side to the cold side without conversion to electricity, effectively reducing the ΔT across the semiconductor material.
- Resulting Decrease in Thermoelectric Performance: Since TEG voltage and power generation are proportional to ΔT, any reduction in ΔT due to heat buildup or thermal bridging reduces the effective temperature gradient and diminishes overall power output and conversion efficiency.
- Mitigation Approaches (Scientific Basis): Filling the spacing with materials of low thermal conductivity (e.g., aerogels, insulating foams) or evacuating the gap to create a vacuum can reduce conduction and convection in the gap, preserving ΔT. Also, mechanical design for thermal isolation: Incorporating thin, thermally insulating spacer layers or coatings can interrupt heat pathways between layers. Thermal Simulation and Experimental Validation: Future studies and simulations should include the effects of interlayer thermal resistance and possible bridging to accurately predict TEG performance under real conditions.

In addition, the 166 TEG layers per meter and constant 2.0 mm gaps are based on the assumption of perfect thermal contact and 0.2 m. Under realistic conditions of HVAC, thermal conduction, and resistance at contact points, ΔT is minimized by thermal bridging, contact resistance, and heat accumulation, and variable temperatures along the pipe are produced by dense layering and ideal performance that are not feasible in the real world unless highly developed thermal management and insulation strategies are employed.

The study clearly indicates that the reported 47% increase in the dimensionless figure of merit (ZT) relies on literature values and theoretically based calculations of BiSbTe with CNT or graphene additives, which imply increased thermoelectric properties. It is the optimization and design of the TEG module based on simulation and not on experimental synthesis or manufacture of these high-technology composite materials. It is therefore accepted that experimental validation, synthesis viability, and long-term performance under operating thermal cycling conditions are the necessary next steps, and they are expected to be undertaken in the future in the context of a future study that is out of the scope of the current study.

The simulation method used focused mainly on the bulk material properties and geometric design, ignoring the crucial interface phenomena, such as contact resistance between the semiconductor legs and copper interconnects. As a result, it

did not take into account the significant impact of contact resistance. The study acknowledges that interface contact resistance can be important and decrease the efficiency of real-world devices, but such quantities cannot be measured without multi-physics modelling and careful experimental characterization. Consequently, contact resistance and interface thermal/electrical resistances are to be introduced into the future refined models and prototype testing phases to reflect closer real performance. The present results, hence, provide an idealized maximum of the performance, a convenient reference with which to optimize the design before addressing losses at the interface.

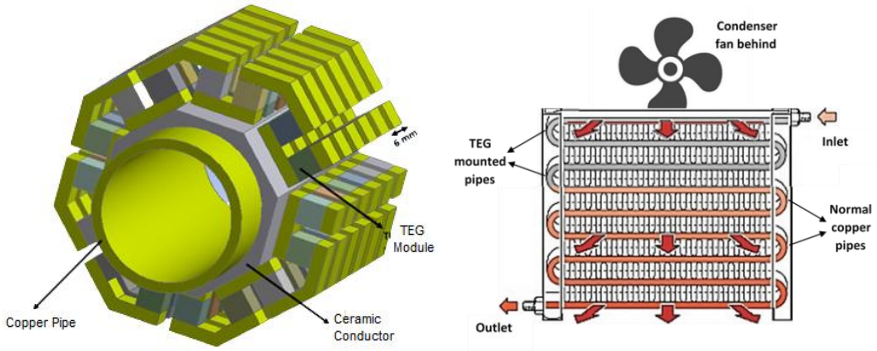

(a) **(b)**

Fig. 12. (a) TEG module mounted on copper pipes, (b) modified condenser with TEG mounted pipes.

Table 7. Power index per meter for the developed design

Temperature gradient in (°C)	Power per layer 7(6 mm) in W	Power per meter in W/m
10	0.01176	1.95
20	0.04702	7.81
30	0.10577	17.56
40	0.18802	31.21

The main objective of the condenser is to cool down the refrigerant, this should be considered when adding the TEG-mounted pipes to the condenser, as the TEGs may reduce the cooling effect. Therefore, it is better to implement the TEG-mounted pipes only in the few upper layers of the condenser pipes, while the rest stays the same. Normally, the width of a domestic condenser is between 25 to 40 cm, and each layer pipe is also around the same length. If just the first 4 layers are replaced with TEG-mounted pipes, then one meter or more will be added. A schematic of adding the TEG-mounted pipes to the condenser is shown in Fig. 12(b).

Power generation from the TEG-mounted pipes is simulated and calculated, and it is shown from the values listed in Table 7 that such generated power is relatively low. As a harvested energy, it is a normal expectation for it to be low and cannot be used to directly drive high or medium-powered applications. A suitable system to utilize this output energy may be developed based on storing the generated power in a battery and then using it afterwards. One convenient candidate application is to invest the harvested power in the air-conditioning unit itself to drive the condenser fan. Figure 13(a) shows

a layout of a power management system at the air conditioning system with the modifications on the electrical circuit of the condenser fan.

The study recognizes that each layer of the TEG generates a small amount of power (between 0.01176 and 0.188 W), which is not enough to run a standard condenser fan that needs 50 to 200 W. Therefore, the suggested system includes a battery buffer that collects energy over time to supply the fan with power when needed.

The study's chosen temperature values for simulation (hot side ~37-67 °C and cold side ~27 °C) correspond well with typical HVAC system operational parameters found in literature and practice, validating the realistic basis of the study's thermal conditions. The temperature values used in this study align well with typical values reported in literature and industry sources for HVAC condenser pipe flow and condenser fan air temperature:

i. Hot side temperature inside the pipe (refrigerant temperature):
   - The articles [25, 26] simulated hot pipe temperatures from about 37 °C to 67 °C, corresponding to temperature gradients of 10 to 40 °C above the cold side (27 °C).
   - Literature and industry sources indicate typical condensing temperature ranges in HVAC systems between approximately 40 °C to 50 °C or higher, depending on conditions - these matches well with the article's nominal range.
   - For example, ambient temperatures plus typical condensing splits (~15-30°F or 8-15 °C) result in condensing temperatures around 45 °C or higher, consistent with the cited 37-67 °C range in the article [27, 28].

ii. Air temperature from the condenser fan (cold side temperature):
   - The article assumes a cold side temperature of about 27 °C (room temperature) to represent the air cooling from the condenser fan.
   - Practical HVAC sources typically consider outdoor ambient air temperature in the range of 20-30 °C, which is consistent with the article's value of 27 °C.
   - The condenser fan blows ambient air to cool the refrigerant pipe, so the cold side temperature being near ambient is realistic [29, 30].
   - The article acknowledges that the harvested power per TEG layer (0.01176 to 0.188 W) is relatively low and insufficient for directly operating a typical condenser fan (50–200 W). Hence, the proposed system incorporates a battery buffer to store energy over time and provide intermittent power to the fan.

The study recommends using TEG-mounted pipes only on the upper layers of the condenser to limit this impact. There is a concern regarding the thermal insulation effect of TEG layers on the condenser pipes that is valid and critically important. Such insulation can reduce heat dissipation effectiveness, leading to higher refrigerant temperatures, lower system COP, and increased compressor workload.

Future research should incorporate detailed thermal performance studies of the modified condenser with TEG layers to balance energy harvesting benefits against any degradation in cooling performance.

As shown in Fig. 13(a), a charging circuit is added between the TEG output wires and the battery. The circuit has voltage regulators along with other electric components to regulate the voltage input to the battery and ensure a one-directional flow. The output of the battery is then input into a control unit. This control unit has electronic switches/gates with a programmable integrated circuit (IC) chip. The

function of this IC chip is to interchange the power source for the condenser fan from the battery to the mains supply and the other way around. The IC chip-switching process depends on the amount of energy stored in the battery. For instance, the IC chip can be programmed to use the battery when its charge reaches 90%. At this point, the mains are disconnected. When the battery drains out and reaches a minimum value of 15%, the IC chip will disconnect the battery from the condenser fan and connect it to the main supply instead. Integrating this system with the condenser has several advantages, including but not limited to, firstly, the compact system and the major component would be the battery. Secondly, the generated power can be stored at any value, and similarly, it can be obtained from the battery at any value, depending on the operating conditions of the fan. Lastly, the overall efficiency can increase significantly [3].

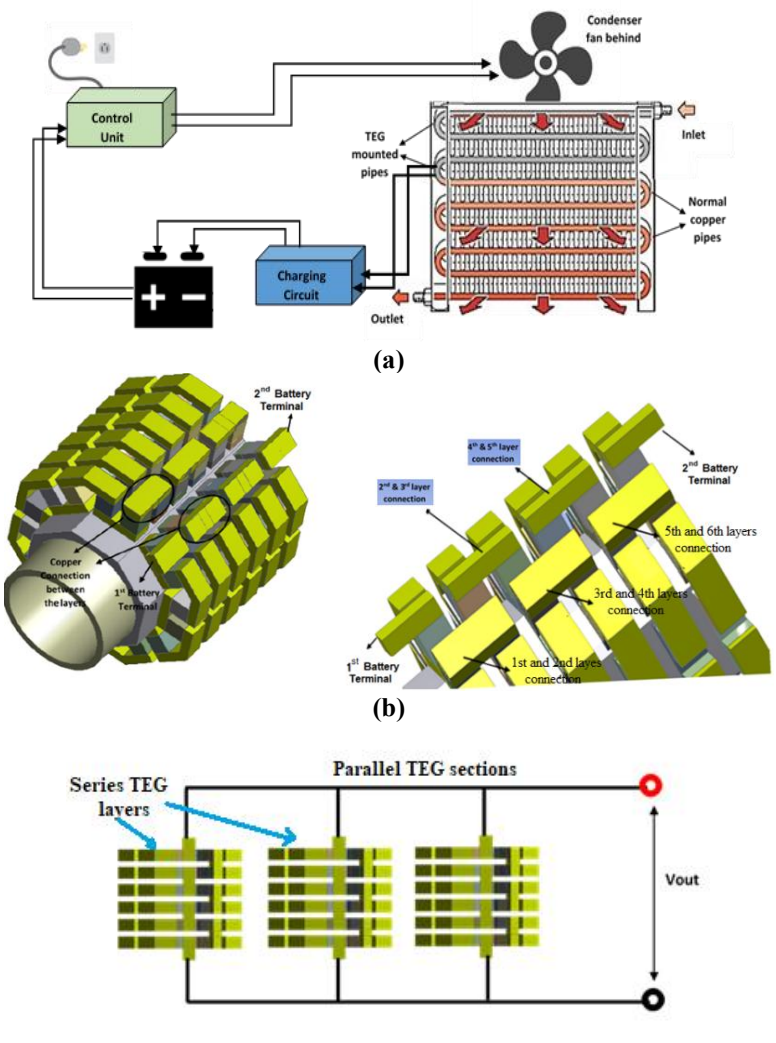

Fig. 13. (a) power management system, (b) connecting the TEG layers in series together with the connections between the layers, (c) series/parallel arrangement for TEG modules.

An important aspect to be considered is the way that the TEG layers are connected, in series or parallel. This aspect can lead to assessing the economic viability of the project. If they were connected in parallel and each layer would be directly connected to the battery through the junctions at the end of each layer, then the voltage would be low, but the current would increase per layer. However, when connecting the TEG layers in series, this will increase the voltage for the same current shown in Fig. 13.

The appropriate number of layers connected in series depends on the voltage required for the battery. The voltage outcome of one layer is from 0.01576 to 0.06304 V, depending on the temperature gradient (from 10 to 40). The voltage outcome of several layers would be the voltage of one layer multiplied by the number of layers. To get a constant value of 5 V out of the minimum temperature gradient of 10°C, then around 320 layers connected in series are needed. There are 166 layers per meter as calculated before, so this means around two meters of the pipes are needed to generate 5 V when the temperature gradient is 10°C. While 80 layers and a 0.5m length are sufficient to produce the 5V, if the temperature gradient is 40°C. A summary of the length and layers needed for each temperature gradient is shown in Table 8.

Table 8. Needed number of layers and length for 5V output.

Temperature gradient	Number of layers for 5V output	Length for 5V output
10	318	2.0 m
20	159	1.0 m
30	105	0.75 m
40	80	0.5 m

The voltage regulator in the charging circuit will adapt the appropriate voltage to be supplied to the battery. If several series layers are to be connected in parallel to increase the current at a desired voltage setting, then the equivalent circuit would be as shown in Fig. 13(c). The voltage and current needed are battery-dependent and based on the requirements of the battery charging power. The number of layers, length and connection type can be determined according to the proposed design.

3.3. Validation and comparison with literature

The current study was theoretical and has not been experimentally proven. Therefore, it was compared with other studies from literature to validate the proposed system. Of course, this comparison may not be entirely fair, given the differences in systems and operating temperature ranges. The relationship between current and power was chosen to characterize the system, as shown on Fig. 14. The figure plots power (W) versus current (D) for three thermoelectric generator (TEG) systems. It compares the performance of the systems from Meng et al. (2016) [31], Junior et al. (2018) [32], and the current study. The graph shows that the power output increases with current for all systems. TEG in Junior's study appears to generate more power at a given current than in the other two studies due to its reliance on operation at temperatures above 40 °C. The results of the current study fall between the two previous studies and yield good power, indicating an improvement in system performance or efficiency.

The Meng et al. (2016) paper works on a full Multiphysics model of the automobile exhaust thermoelectric generators (TEGs), consisting of a real exhaust heat source and a real water-cooling heat sink. It emphasizes that counterflow cooling minimizes the non-uniformity of temperatures between thermoelectric units, which increases the reliability of the system. The dividend power does not necessarily increase with an increased number of TE units because of temperature falls and lateral heat conductors. With constant exhaust channel length, output power optimization is achieved by changing the number of TE units and spacing, optimizing performance at lower material consumption. The results are in the advancement of the design optimization of the waste heat recovery in vehicles.

The design of the study by Junior et al. (2018) describes a new thermoelectric generator (TEG) system of waste heat recovery in the industrial process, which involves the use of 20 INBC1-127.08HTS modules. It recorded a linear voltage against temperature of VOC = 0.4306 Dt and an internal resistance of 9.41 - 0.77 Ω. At 80 °C the temperature gradient offered the highest power output of around 29W on the prototype. The system is characterized by modularity, flexibility, and efficient cogeneration of clean energy using residual heat to reuse, which has proven to be technically viable and can be applied in industries that involve heat exchange processes. This technology has a promise of generating clean and sustainable energy.

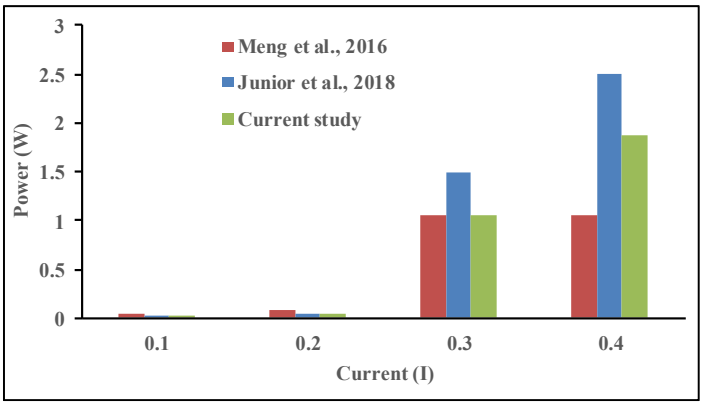

Fig. 14. Validation and comparison of current study results with literature.

It should be stressed that even though absolute values of power depend on the working conditions (e.g., temperature), the fundamental physical behavior is identical: the greater the current, the greater the power output. This is the proper imitation of the fundamental trend, which gives a basis of validation. The findings of the present research are also logically within the two benchmarks. The model is superior to a complex automotive system (Meng et al.) and inferior to a high-temperature industrial system (Junior et al.). This logical stance implies that the predictions of this model are physically sensible, and they do not have an anomalous nature. The comparison shows how it could be improved in terms of performance in its particular design context.

3.4. Limitations

There are several challenges in the proposed system that need to be resolved, requiring additional long-term experiments, material optimization, system

integration, and cost-effective manufacturing processes. Overcoming these limitations is critical to increasing the use of TEGs in HVAC. These solutions must meet the commercial requirements for such systems in terms of cost and compete with currently available systems. Although the proposed design is promising and the results presented are positive, some limitations must be considered regarding the use and development of this system:

Power Density Challenges: The power density ranges from 0.01176 to 0.18802 watts, which is relatively low, preventing its use in high-power applications without additional energy storage and management.

Integration Impacts on HVAC System Efficiency: By installing multiple layers of TEGs on the condenser tube, there is the potential to compromise the heat transfer efficiency and refrigerant volume of the HVAC system, leading to a decrease in overall performance if installed or constructed in an imperfect manner. Material and Fabrication Complexity: Manufacturing a cylindrical thermoelectric generator (TEG) requires precise milling and assembly of materials, which can increase material and fabrication complexity, and thus costs, compared to standard rectangular modules.

Sensitivity to Thermal Gradient: Efficiency and power output are highly dependent on the temperature difference between the hot and cold sides. A combination of small or irregular thermal gradients can result in unsatisfactory power capture.

Durability and Environmental Concerns: Materials must be selected, where possible, to ensure durability under a variety of potential environmental conditions, mechanical loads, and fluctuating temperatures within HVAC systems. Pilot testing must be conducted to determine near-term reliability.

Scalability and Installation Constraints: Multiple layers of TEGs on long tubes had to be developed for mechanical integrity and to accommodate the spatial limitations of the HVAC system they are mounted on. Complexity of power management systems: The design requires a highly sophisticated energy storage and control system to handle the low-power pulses generated by this array of thermoelectric generators, which adds additional engineering and maintenance issues.

4. Conclusions

This study addresses energy harvesting by developing a system to recover wasted heat from air conditioning units using TEG materials. The design optimizes heat capture in the condenser, where the refrigerant accumulates heat post-compressor. TEG modules, specifically designed for cylindrical pipes, are integrated onto copper pipes within the condenser. Material selection involves the top options for P-type and N-type semiconductors, resulting in nine combinations. Simulations cover voltage inputs and temperature differences relevant to air-conditioning systems. It is worth noting that the best blend of thermoelectric materials yielded power per TEG layer of 0.01176 watts at the lowest temperature difference of 10 °C, and 0.18802 watts per TEG layer at a temperature difference of 40 °C. Further considerations involve integrating the TEG-piped design into the condenser, managing electrical connections, and exploring energy storage options. The study proposes using the generated power to drive the condenser fan, with the potential for storing excess energy in a battery. While TEG-based thermal energy harvesting

is not new, this study introduces a unique design accommodating cylindrical pipe geometry, demonstrating its adaptability for various applications beyond air conditioning units. The study suggests possibilities for improvement, such as integrating heat sinks for enhanced cooling, which could significantly boost efficiency and power generation.

While the developed design's primary application is air conditioning units, its adaptability makes it suitable for various scenarios featuring hot pipes. This includes domestic water heating systems and any setting involving hot and cold fluids.

Disclosure of interest

We the authors declare no affiliations with or involvement in any organization or entity with any financial interest (such as honoraria; educational grants; participation in speakers' bureaus; membership, employment, consultancies, stock ownership, or other equity interest; and expert testimony or patent licensing arrangements), or non-financial interest (such as personal or professional relationships, affiliations, knowledge or beliefs) in the subject matter or materials discussed in this manuscript.

Conflict of Interests

The authors declare that there is no conflict of interests regarding the publication of this brief note.

Data Availability

The research data is available upon request. To request the data, contact the first author of the article.

Acknowledgement

The authors gratefully acknowledge the publication support provided by the Institution of Mechanical Engineers (IMechE), UK, through the SEAR Mini Research Grant, and by Universiti Tenaga Nasional through the BOLD Research Grant 2024 (BOLD2024), Grant No. J510051055.

References

1. Azam, M.W.; Chaudhary, G.Q.; Sajjad, U.; Abbas, N.; and Yan, W.-M. (2023). Performance investigation of solar assisted desiccant integrated Maisotsenko cycle cooler in subtropical climate conditions. *Case Studies in Thermal Engineering*, 44, 102864.
2. Xi, H.; Luo, L.; and Fraisse, G. (2007). Development and applications of solar-based thermoelectric technologies. *Renewable and Sustainable Energy Reviews*, 11(5), 923-936.
3. Kabeel, A.; Abdelgaied, M.; Zakaria, Y.; and Sathyamurth, R. (2018). Performance improvement of a solar assisted desiccant air conditioning coupled with condenser for water production. *Proceedings of the* 2018 9*th International Renewable Energy Congress* (*IREC*), Hammamet, Tunisia, 1-6.

4. Ma, Z.; Ren, H.; and Lin, W. (2019). A review of heating, ventilation and air conditioning technologies and innovations used in solar-powered net zero energy Solar Decathlon houses. *Journal of Cleaner Production*, 240, 118158.
5. Malik, A.S. et al. (2018). Smart grid scenarios and their impact on strategic plan - A case study of Omani power sector. *Sustainable Cities and Society*, 37, 213-221.
6. Al-Waeli, A.H.; Kazem, H.A.; Chaichan, M.T.; and Sopian, K. (2021). A review of photovoltaic thermal systems: Achievements and applications. *International Journal of Energy Research*, 45(2), 1269-1308.
7. Aridi, R.; Faraj, J.; Ali, S.; Lemenand, T.; and Khaled, M. (2021). Thermoelectric power generators: state-of-the-art, heat recovery method, and challenges. *Electricity*, 2(3), 359-386.
8. Sil, I.; Mukherjee, S.; and Biswas, K. (2017). A review of energy harvesting technology and its potential applications. *Environmental and Earth Sciences Research Journal*, 4(2), 33-38.
9. Champier, D. (2017). Thermoelectric generators: A review of applications. *Energy Conversion and Management*, 140, 167-181.
10. Goh, S.Y.; and Kok, S.L. (2017). Electrical energy harvesting from thermal energy with converged infrared light. *In IOP Conference Series*: *Materials Science and Engineering*, 210(1), 012039.
11. Gkoumas, K.; Petrini, F.; and Bontempi, F. (2017). Piezoelectric vibration energy harvesting from airflow in HVAC (heating ventilation and air conditioning) systems. *Procedia Engineering*, 199, 3444-3449.
12. Fiorentini, M.; Cooper, P.; and Ma, Z. (2015). Development and optimization of an innovative HVAC system with integrated PVT and PCM thermal storage for a net-zero energy retrofitted house. *Energy and Buildings*, 94, 21-32.
13. LeBlanc, S. (2014). Thermoelectric generators: Linking material properties and systems engineering for waste heat recovery applications. *Sustainable Materials and Technologies*, 1-2, 26-35.
14. Jouhara, H. et al. (2018). Waste heat recovery technologies and applications. *Thermal Science and Engineering Progress*, 6, 268-289.
15. Mona, Y.; Chaichana, C.; Rattanamongkhonkun, K.; and Thiangchanta, S. (2022). Energy harvesting from air conditioners by using a thermoelectric application. *Energy Reports*, 8, 456-462.
16. Chen, J.F.; Zhang, L.; and Dai, Y.J. (2018). Performance analysis and multi-objective optimization of a hybrid photovoltaic/thermal collector for domestic hot water application. *Energy*, 143, 500-516.
17. Yang, C.-J.; Yang, T.-C.; Chen, P.-T.; and Huang, K.D. (2019). An innovative design of regional air conditioning to increase automobile cabin energy efficiency. *Energies*, 12(12), 2352.
18. Kumar, P.M. et al. (2019). The design of a thermoelectric generator and its medical applications. *Designs*, 3(2), 22.
19. Park, J.G.; and Lee, Y.H. (2016). High thermoelectric performance of Bi-Te alloy: Defect engineering strategy. *Current Applied Physics*, 16(9), 1202-1215.
20. Li, J.-F.; Liu, W.-S.; Zhao, L.-D.; and Zhou, M. (2010). High-performance nanostructured thermoelectric materials. *NPG Asia Materials*, 2(4), 152-158.

21. Yang, L.; Chen, Z.-G.; Dargusch, M.S.; and Zou, J. (2018). High performance thermoelectric materials: progress and their applications. *Advanced Energy Materials*, 8(6), 1701797.
22. Jouhara, H. et al. (2021). Thermoelectric generator (TEG) technologies and applications. *International Journal of Thermofluids*, 9, 100063.
23. Alexander, C.K.; and Sadiku, M.N.O. (2007). *Fundamentals of electric circuits*. McGraw-Hill Higher Education, Boston, USA.
24. Demir, M.E.; and Dincer, I. (2017). Performance assessment of a thermoelectric generator applied to exhaust waste heat recovery. *Applied Thermal Engineering*, 120, 694-707.
25. Han, C.; Li, Z.; and Dou, S. (2014). Recent progress in thermoelectric materials. Chinese Science Bulletin, 59, 2073-2091.
26. Huang B.; and Shen Z.-G. (2022). Performance assessment of annular thermoelectric generators for automobile exhaust waste heat recovery. Energy, 246, 123375.
27. Guo, Q.; Everage, D.; and Zhang, Q. (2024). Hands-on learning for enhanced thermodynamics education with refrigeration system analysis. *Proceedings of the ASME International Mechanical Engineering Congress and Exposition*, Portland, Oregon, USA, 88650, V007T09A042.
28. Dincer, I.; and Kanoglu, M. (2010). *Refrigeration systems and applications*. Wiley.
29. Naphon, P. (2010). On the performance of air conditioner with heat pipe for cooling air in the condenser. *Energy Conversion and Management*, 51(11), 2362-2366.
30. Eidan, A.A.; Alshukri, M.J.; Al-fahham, M.; AlSahlani, A.; and Abdulridha, D.M. (2021). Optimizing the performance of the air conditioning system using an innovative heat pipe heat exchanger. *Case Studies in Thermal Engineering*, 26, 101075.
31. Meng, J.-H.; Wang, X.-D.; and Chen, W.-H. (2016). Performance investigation and design optimization of a thermoelectric generator applied in automobile exhaust waste heat recovery. *Energy Conversion and Management*, 120, 71-80.
32. Junior, O.H.A.; Calderon, N.H.; and Souza, S.S.D. (2018). Characterization of a thermoelectric generator (TEG) system for waste heat recovery. *Energies*, 11(6), 1555.